crystals

MDPI

Article

Performance Improvement of InGaN-Based LEDs via a Current-Blocking Region Prepared via Hydrogen Passivation

Pavel Kirilenko [1], Cesur Altinkaya [2], Daisuke Iida [1] and Kazuhiro Ohkawa [1,*]

[1] Electrical and Computer Engineering Program, Computer, Electrical and Mathematical Sciences and Engineering Division, King Abdullah University of Science and Technology (KAUST), Thuwal 23955-6900, Saudi Arabia
[2] Material Science and Engineering Program, Physical Sciences and Engineering Division, King Abdullah University of Science and Technology (KAUST), Thuwal 23955-6900, Saudi Arabia
* Correspondence: kazuhiro.ohkawa@kaust.edu.sa

Abstract: We report p-GaN passivation via hydrogen plasma used to create current blocking regions (CBRs) in InGaN-based green LEDs with standard dimensions of 280 × 650 μm^2. The CBRs are created before mesa etching in two variants: underneath the opaque metal p-pad and both underneath the p-pad and along the device's mesa perimeter. The peak EQE increased by 13% and 23% in the first and the second cases, respectively, in comparison to the reference LED with no CBR. With a high injection current of 50 A/cm^2, the EQE value increased by 2% in the case of CBRs underneath the p-pad as well as by 14% in the case of CBRs both underneath the p-pad and along the mesa perimeter (relative to the reference sample with no CBR).

Keywords: InGaN; LED; current blocking layer; hydrogen passivation; injection efficiency; light extraction efficiency; reactive ion etching

Citation: Kirilenko, P.; Altinkaya, C.; Iida, D.; Ohkawa, K. Performance Improvement of InGaN-Based LEDs via a Current-Blocking Region Prepared via Hydrogen Passivation. *Crystals* **2022**, *12*, 1733. https://doi.org/10.3390/cryst12121733

Academic Editor: Paul J. Simmonds

Received: 23 October 2022
Accepted: 24 November 2022
Published: 1 December 2022

1. Introduction

The InGaN-based light-emitting diodes (LEDs) are one of the most popular light sources with applications in display backlight and indoor or outdoor light sources [1–3]. Despite the remarkable efficiency of blue InGaN LEDs, longer wavelength-emitting devices suffer from internal quantum efficiency reductions due to In concentrations in the active region's InGaN alloy [4]. This makes it necessary to seek ways to improve the external quantum efficiency via optimization of the charge carrier injection and light extraction efficiencies.

The conventional method of device fabrication for the InGaN LEDs grown on an insulating sapphire substrate is mesa etching. In this device configuration, the p- and n-electrodes of the device are both situated on the same side of the chip [5]. The conventional structural schematics are shown in Figure 1a. However, the metal p-pad position on top of the device's mesa inevitably reduces the device's light extraction efficiency. The shortest—and therefore least resistive—path for the hole injection lies right underneath the metal p-pad. The most intense light emission, especially at the lower injection currents, occurs there and is re-adsorbed by the metal pad above.

Several solutions have been provided to solve the problem of light adsorption by the metal p-pad. The common idea among them is to block the current injection right underneath the metal p-pad. A current blocking layer (CBL) can be introduced underneath the transparent electrode layer. In most cases, the CBL consists of an insulating layer (conventionally SiO_2) that is either smooth [6] or patterned [7]. This method, depending on the initial total surface occupied by the metal p-pad, provides up to a 60% improvement [6] in the device's light output power versus similar LEDs without a CBL. Another approach to hole injection patterning can be realized using the selective activation of p-GaN [8]. A 10% increase in light output power was achieved in this way. The current injection patterning was equally achieved by the device's p-side exposure to the oxygen plasma, making it insulate. In this case, the additional InGaN thin layer is deposited on top of the p-GaN layer and is converted into Ga_2O_3 in the presence of oxygen plasma. This leads to the InGaN LED output power improvement ranging from 10% [9] to 17% [10] at 60 mA forward current injection. Summarizing the different approaches to the CBL formation, in its principle it results in the current injection patterning by the formation of the high-resistive regions in the chosen regions of the LED surface.

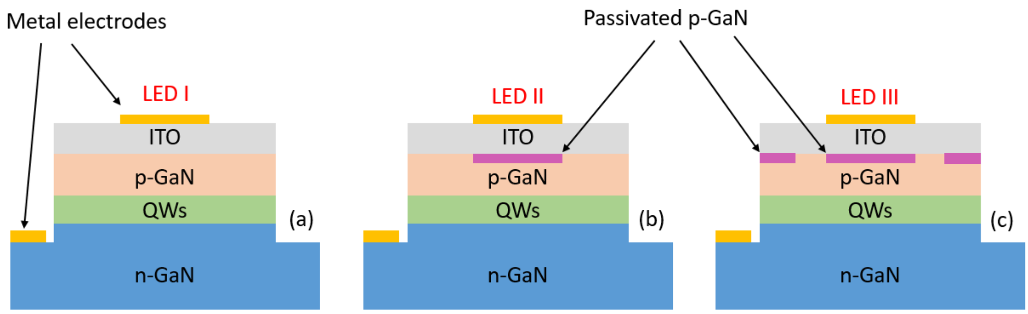

Figure 1. Experimental LEDs cross-section schematics in case of (**a**) LED I—reference LED; (**b**) LED II—LED with the hydrogen passivation applied under the electrode; (**c**) LED III—LED with the hydrogen passivation applied under the electrode and along the mesa perimeter.

We therefore utilized an approach that is rather similar to the selective activation of p-GaN. We selectively increased the resistivity of p-GaN via Mg-dopant deactivation and a hydrogen plasma. After plasma exposure, the p-GaN sheet resistance increases up to ten-fold [11,12]. We previously applied hydrogen passivation to achieve mesa etching-free pixelization of InGaN LED [11,13] and micro-LED sidewall passivation [14]. Here, we used hydrogen passivation to suppress the current injection underneath the metal p-pad of the LED chip. Two versions of the hydrogen passivation pattern were explored here. The first version is, as described above, a current blocking region (CBR) underneath the p-pad. The second version adds a CBR along the device's mesa perimeter. Schematics of these designs are present in Figure 1b,c. Below, we will refer to the experimental samples as LED I in the case of the reference sample, LED II for the chip with a CBR underneath the p-pad, and LED III in the case of the CBR both underneath the p-pad and along the device's mesa perimeter. The additional current-blocking region along the mesa perimeter in the case of LED III is introduced to suppress the non-radiative recombination of the charge carriers in the mesa sidewall region. Non-radiative recombination occurs in the material defects introduced during mesa formation via reactive ion etching [15–17]. Suppression of the current injection into the LED sidewall region can further improve device efficiency with only a minor decrease in the chip total area.

2. Materials and Methods

Commercial green InGaN LED wafers were utilized. These LEDs are grown on a *c*-plane sapphire substrate with a 2-μm-thick unintentionally doped GaN template. The LED's active region consists of 16 periods of InGaN/GaN quantum wells. The devices' n- and p- sides have Si- and Mg-doped GaN, respectively.

After standard wafer de-greasing and cleaning, Ti/Au alignment marks were deposited using direct current (DC) sputtering with patterning performed by photolithography and lift-off. This procedure aligns the passivated p-GaN regions with further mesa etching. The additional alignment marks are needed because the hydrogen passivation leaves close to no observable pattern on the p-GaN surface. After the alignment marks are completed, the p-GaN surface is covered with a thin (100 nm) layer of SiO_2 by plasma-enhanced chemical vapor deposition (PECVD) followed by the pattern transfer via photolithography. The oxide layer is then selectively etched using C_4F_8 reactive ion etching (RIE), thus exposing the p-GaN areas designed to be passivated.

After removing the remaining photoresist, the wafers were exposed to hydrogen plasma via a PECVD chamber. The plasma exposure was conducted for 4 min with an RF power of 250 W and at a substrate temperature of 300 °C. This step is the most critical, and the shape of the hydrogen passivation pattern is the only difference in the device processing of LED I, II, and III (Figure 1).

LED I has no passivation and is a reference sample. LED II has a passivated p-GaN underneath the device's p-electrode. The geometry of the CBR is almost completely similar to that with a p-pad with an important addition of the 2.5 µm-wide indent in every direction. In this way, for example, the segment of the metal p-pad that consists of a straight line with a thickness of 5 µm is followed by a 10 µm-wide current-blocking region. LED III has a passivated p-GaN indent along the device's mesa perimeter with a width of 10 µm in addition to the same passivated region underneath the contact as in the case of LED II. The SiO_2 mask is later removed with a hydrofluoric acid-based buffered oxide etchant (BOE).

All experimental wafers were treated similarly after the hydrogen passivation step was complete. The 90-nm-thick indium tin oxide (ITO) layer was then deposited by an e-beam evaporator followed by a two-step annealing process [18]. The mesa pattern was then transferred on top of the ITO by photolithography. The mesa etching was performed via Cl_2 RIE, and the total resulting mesa depth was 800 nm. The device sidewalls were then treated with tetramethylammonium hydroxide (TMAH) wet etching at room temperature for 40 min. The Cr/Pt/Au electrodes were then sputtered and patterned using a lift-off technique.

The resulting devices were characterized on a probe station equipped with an integrating sphere and a spectrometer. The light output measurements used an integrating sphere mounted on top of the wafer with the input window aligned to the characterized LED. These measurements were performed on the same height and LED orientation, which allowed us to compare the light output characteristics of the different wafers. However, we operated in terms of on-wafer measurements because the device was not completely inserted into the integration sphere. The wire bonding captured the EL images using an optical microscope and resulted in the operating LED pictures (Figure 2).

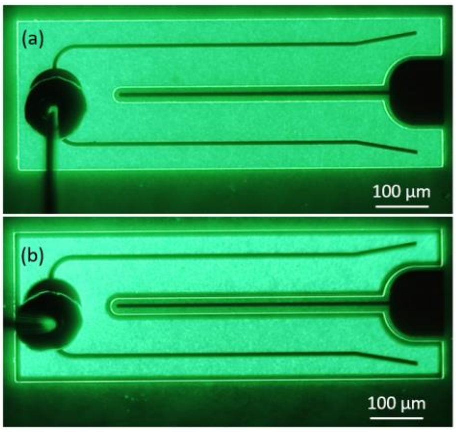

Figure 2. Microscope images of LEDs with the injected current of 3 mA: (**a**) LED I; (**b**) LED III.

The current injection suppression into selected regions resulted in the device's different active areas. To normalize the current density, the active areas of 194,944, 171,358, and 138,797 µm^2 were used for LED I, II, and III, respectively.

3. Results

Figure 2 shows optical microscope images of the LEDs with the fixed forward current injection of 3 mA. Figure 2a demonstrates the reference chip design of LED I. Figure 2b shows LED III. LED II is not present because its electroluminescence intensity distribution is not different from that of LED I. LED III is more illustrative in this case because the

CBR is visible as a dimmed frame along the perimeter of the device mesa. This serves as a proof of the concept and secures the assumption that the electroluminescence is suppressed in the current-blocking region underneath the metal p-pad. However, as is described in the materials and methods, the CBR underneath the p-pad has a 2.5-μm indent in every direction. This widening is also observable in Figure 2b.

The device *I-V* behavior is seen in Figure 3. The linear fit in the voltage range [2.5:3] V was used to extract the differential resistance R_d and forward voltage V_f for the measured chips. The resulting value of V_f = 2.25 V, equal for all three LEDs, agrees well with the emission peak wavelength of approximately 530 nm. The value of R_d decreases from 15.02 Ω in the case of LED I to 14.95 Ω and 14.53 Ω in the case of LED II and LED III, respectively.

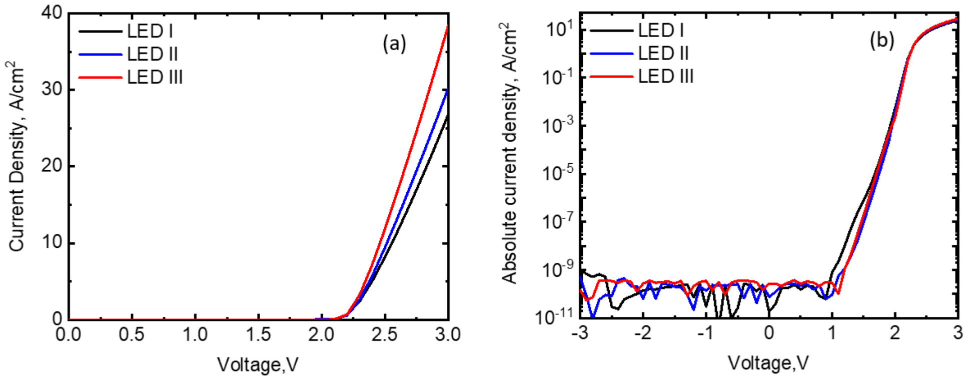

Figure 3. *I-V* characteristics of the experimental LEDs with current plotted in (**a**) linear scale and (**b**) logarithmic scale.

Under the reverse bias of down to −3 V, all three experimental LEDs show the low current in the order of 10^{-10} A/cm^2, as is shown in Figure 3b. This fact illustrates that the introduction of the CBR structures does not affect the device's leakage current.

On-wafer light output power measurement results are shown in Figure 4. With a high injection current of 50 A/cm^2, the measured power was 3.9, 3.96, and 4.13 mW for LED I, LED II, and LED III, respectively. The light output power improvement in the case of LED II is mostly due to the suppression of the light adsorption by the opaque p-pad. The derivative value of the on-wafer EQE is shown in Figure 5. For easier comparison, the EQE peak position and value along with efficiency at 50 A/cm^2 forward current injection is provided in Table 1. The peak EQE improvement in comparison with the reference sample is also present in Table 1.

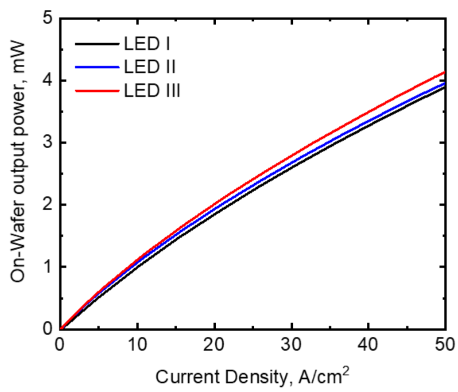

Figure 4. On-wafer *L-I* of experimental LEDs.

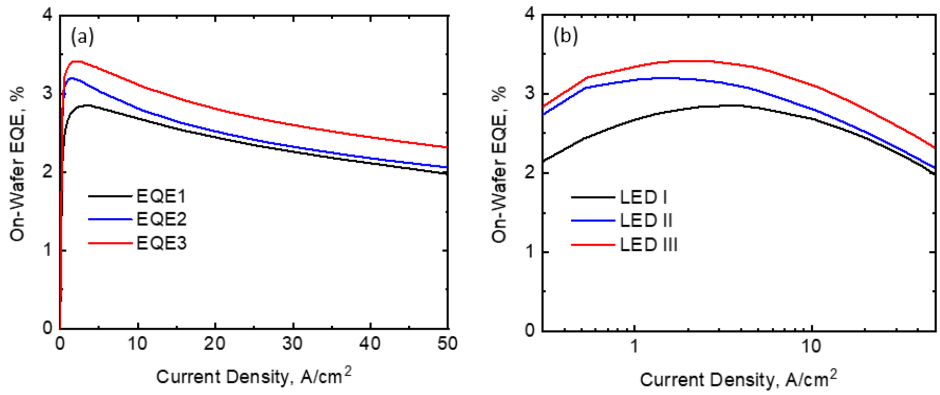

Figure 5. On-wafer EQEs of experimental LEDs with current plotted in (**a**) linear scale and (**b**) logarithmic scale.

Table 1. Characterization of on-wafer EQE behavior.

Value	LED I	LED II	LED III
On-wafer EQE peak position, A/cm^2	4.61	1.58	2.16
On-wafer EQE peak value, %	2.85	3.2	3.41
On-wafer EQE @50 A/cm2, %	1.98	2.02	2.32
Peak EQE improvement, comparing to LED I, %	-	12.3	19.6

4. Discussion

In the first case—when the CBR is introduced underneath the metal p-pad—the efficiency improvement relative to reference sample was most pronounced in the low-current region. However, in the high-current region, LED I and LED II behaved almost identically in terms of the EQE. In the second case, when the CBR was additionally introduced along the mesa perimeter, we observed consistent EQE gains of LED III versus LED II.

The LED EQE improvement in the case of LED II was mostly due to a reduction in the current crowding effect [19,20]. CBR consists of passivated p-GaN and assists in current spreading away from the opaque p-pad. This effect boosts the peak EQE in the low-current region. The current density lateral distribution becomes more even with a higher injection current. The EQEs of LED I and LED II are asymptotically similar. For example, at an injection current of 50 A/cm^2, the EQE gain by CBR underneath the p-pad is only 2% versus the reference sample with no CBR. The efficiency drop in the high current injection region is determined mostly by the high-order terms of the internal quantum efficiency (IQE) in this case [21].

The EQE improvement of up to 19.6% in the case of LED III is most likely not caused by the IQE factor of the EQE. A reduced leakage current along the device's sidewalls leads to improvements in the injection efficiency. An efficiency gain with the same order of magnitude was reported in the case of the standard-size LED sidewall passivation via a dielectric layer deposition on the mesa sidewall [22] and a micro-LED sidewall passivation by hydrogen plasma [14]. We assume that the great improvement in the device's light output density, and, therefore, its efficiency, was brought about by the reduction in the non-radiative recombination that occurred on the device sidewalls [23]. We achieved that by current injection suppression along the device mesa.

The technology of hydrogen passivation has shown versatile applications and can be implemented for various types of LED devices. To check the technology reliability, the similarly fabricated device went through the durability test, as was shown in the previous work of our group [11]. There, the device's light output density was measured during the prolonged operation under 11.6 A/cm^2 and 116 A/cm^2 forward current injections. For the 100 h of the durability experiment, the light output density did not drop on either level of current injection.

5. Conclusions

In this experiment, p-GaN selective passivation via hydrogen plasma was utilized to improve the external quantum efficiency of the standard-size green InGaN LED. Before ITO deposition and device mesa etching, current-blocking regions were applied to the LED's Mg-doped p-side. Two different CBR designs were applied. In the first one, current injection was suppressed underneath the metal p-pad. In the second one, current injection was suppressed both underneath the metal p-pad and along the mesa perimeter. The resulting selective current injection was directly observed via optical microscopy. With the CBR both underneath the metal pad and along the mesa perimeter, the peak EQE value increased 1.23 times versus the reference sample with no CBR introduced. The EQE peak position with respect to the injected current shifted from 9 mA to 4 mA. CBR formation via hydrogen passivation applied to LEDs with a peak emission wavelength of any value as long as a hole injection was provided by GaN: Mg. This is highly useful for the III-nitride LEDs with low IQE (emitting in the yellow-red part of the spectrum). The CBR formation technique was easily introduced into the device fabrication pipeline because this fabrication step occurs before the regular lateral-chip LED fabrication routine.

Author Contributions: Conceptualization, P.K., D.I. and K.O.; methodology, P.K. and D.I.; validation, P.K., D.I. and K.O.; formal analysis, C.A.; investigation, P.K. and C.A.; resources, P.K. and D.I.; data curation, P.K. and C.A.; writing—original draft preparation, P.K.; writing—review and editing, D.I.; visualization, P.K.; supervision, K.O.; project administration, P.K. and D.I.; funding acquisition, K.O. All authors have read and agreed to the published version of the manuscript.

Funding: King Abdullah University of Science and Technology (BAS/1/1676-01-01).

Data Availability Statement: Data underlying the results presented in this paper are not publicly available at this time but may be obtained from the authors upon reasonable request.

Acknowledgments: The fabrication processes in this work were supported by Nanofabrication Core Lab.

Conflicts of Interest: The authors declare no conflict of interest.

References

1. Steigerwald, D.A.; Bhat, J.C.; Collins, D.; Fletcher, R.M.; Holcomb, M.O.; Ludowise, M.J.; Martin, P.S.; Rudaz, S.L. Illumination with solid state lighting technology. *IEEE J. Sel. Top. Quantum Electron.* **2002**, *8*, 310–320. [CrossRef]
2. Krames, M.R.; Shchekin, O.B.; Mueller-Mach, R.; Mueller, G.; Zhou, L.; Harbers, G.; Craford, M.G. Status and Future of High-Power Light-Emitting Diodes for Solid-State Lighting. *J. Disp. Technol.* **2007**, *3*, 160–175. [CrossRef]
3. Crawford, M.H. LEDs for Solid-State Lighting: Performance Challenges and Recent Advances. *IEEE J. Sel. Top. Quantum Electron.* **2009**, *15*, 1028–1040. [CrossRef]
4. Damilano, B.; Gil, B. Yellow–red emission from (Ga, In)N heterostructures. *J. Phys. D Appl. Phys.* **2015**, *48*, 403001. [CrossRef]
5. Nakamura, S.; Mukai, T.; Senoh, M. Candela-class high-brightness InGaN/AlGaN double-heterostructure blue-light-emitting diodes. *Appl. Phys. Lett.* **1994**, *64*, 1687–1689. [CrossRef]
6. Huh, C.; Lee, J.-M.; Kim, D.-J.; Park, S.-J. Improvement in light-output efficiency of InGaN/GaN multiple-quantum well light-emitting diodes by current blocking layer. *J. Appl. Phys.* **2002**, *92*, 2248–2250. [CrossRef]
7. Park, J.-S.; Sung, Y.H.; Na, J.-Y.; Kang, D.; Kim, S.-K.; Lee, H.; Seong, T.-Y. Use of a patterned current blocking layer to enhance the light output power of InGaN-based light-emitting diodes. *Opt. Express* **2017**, *25*, 17556–17561. [CrossRef]
8. Chia-Ming, L.; Chang-Cheng, C.; Yu-Chuan, L.; Chen, I.L.; Jen-Inn, C. InGaN-GaN MQW LEDs with current blocking layer formed by selective activation. *IEEE Electron Device Lett.* **2004**, *25*, 384–386. [CrossRef]
9. Lee, K.H.; Kang, K.M.; Hong, G.C.; Kim, S.H.; Sun, W.Y.; Yang, G.M. Improved Light Extraction of GaN-Based Light-Emitting Diodes by an Ion-Damaged Current Blocking Layer. *Jpn. J. Appl. Phys.* **2012**, *51*, 082102. [CrossRef]
10. Lee, K.H.; Moon, Y.T.; Oh, S.K.; Kwak, J.S. High Efficiency and ESD of GaN-Based LEDs With Patterned Ion-Damaged Current Blocking Layer. *IEEE Photonics Technol. Lett.* **2015**, *27*, 149–152. [CrossRef]
11. Zhuang, Z.; Iida, D.; Velazquez-Rizo, M.; Ohkawa, K. Ultra-small InGaN green micro-light-emitting diodes fabricated by selective passivation of p-GaN. *Opt. Lett.* **2021**, *46*, 5092–5095. [CrossRef]
12. Polyakov, A.Y.; Smirnov, N.B.; Govorkov, A.V.; Baik, K.H.; Pearton, S.J.; Luo, B.; Ren, F.; Zavada, J.M. Hydrogen plasma passivation effects on properties of p-GaN. *J. Appl. Phys.* **2003**, *94*, 3960–3965. [CrossRef]
13. Zhuang, Z.; Iida, D.; Ohkawa, K. Ultrasmall and ultradense InGaN-based RGB monochromatic micro-light-emitting diode arrays by pixilation of conductive p-GaN. *Photon. Res.* **2021**, *9*, 2429–2434. [CrossRef]

14. Kirilenko, P.; Iida, D.; Zhuang, Z.; Ohkawa, K. InGaN-based green micro-LED efficiency enhancement by hydrogen passivation of the p-GaN sidewall. *Appl. Phys. Express* **2022**, *15*, 084003. [CrossRef]
15. Zhuang, Z.; Iida, D.; Ohkawa, K. Effects of size on the electrical and optical properties of InGaN-based red light-emitting diodes. *Appl. Phys. Lett.* **2020**, *116*, 173501. [CrossRef]
16. Yu, H.; Memon, M.H.; Wang, D.; Ren, Z.; Zhang, H.; Huang, C.; Tian, M.; Sun, H.; Long, S. AlGaN-based deep ultraviolet micro-LED emitting at 275 nm. *Opt. Lett.* **2021**, *46*, 3271–3274. [CrossRef]
17. Bulashevich, K.A.; Karpov, S.Y. Impact of surface recombination on efficiency of III-nitride light-emitting diodes. *Phys. Status Solidi (RRL)–Rapid Res. Lett.* **2016**, *10*, 480–484. [CrossRef]
18. Zhuang, Z.; Iida, D.; Kirilenko, P.; Velazquez-Rizo, M.; Ohkawa, K. Optimal ITO transparent conductive layers for InGaN-based amber/red light-emitting diodes. *Opt. Express* **2020**, *28*, 12311–12321. [CrossRef]
19. Guo, X.; Schubert, E.F. Current crowding in GaN/InGaN light emitting diodes on insulating substrates. *J. Appl. Phys.* **2001**, *90*, 4191–4195. [CrossRef]
20. Li, C.K.; Wu, Y.R. Study on the Current Spreading Effect and Light Extraction Enhancement of Vertical GaN/InGaN LEDs. *IEEE Trans. Electron Devices* **2012**, *59*, 400–407. [CrossRef]
21. Dai, Q.; Shan, Q.; Wang, J.; Chhajed, S.; Cho, J.; Schubert, E.F.; Crawford, M.H.; Koleske, D.D.; Kim, M.-H.; Park, Y. Carrier recombination mechanisms and efficiency droop in GaInN/GaN light-emitting diodes. *Appl. Phys. Lett.* **2010**, *97*, 133507. [CrossRef]
22. Hsu, C.-H.; Chan, Y.-C.; Wei Cheng, C.; Chang, C.-H.; Liou, J.-K.; Cheng, S.-Y.; Guo, D.-F.; Liu, W.-C. Study of GaN-Based LEDs with Hybrid SiO_2 Microsphere/Nanosphere AntiReflection Coating as a Passivation Layer by a Rapid Convection Deposition. *IEEE Trans. Electron Devices* **2017**, *64*, 1134–1139. [CrossRef]
23. Piprek, J. Efficiency droop in nitride-based light-emitting diodes. *Phys. Status Solidi A* **2010**, *207*, 2217–2225. [CrossRef]